Available online at www.sciencedirect.com

SciVerse ScienceDirect

Ceramics International 39 (2013) 7793–7802

CERAMICS INTERNATIONAL

www.elsevier.com/locate/ceramint

How bone marrow-derived human mesenchymal stem cells respond to poorly crystalline apatite coated orthopedic and dental titanium implants

Maryam Ghaffari[a,b], Fathollah Moztarzadeh[b], Azadeh Sepahvandi[b], Masoud Mozafari[b], Shahab Faghihi[a,*]

[a]*Tissue Engineering and Biomaterials Division, National Institute of Genetic Engineering and Biotechnology, Tehran 14965/161, Iran*
[b]*Biomaterials Group, Faculty of Biomedical Engineering (Center of Excellence), Amirkabir University of Technology, P. O. Box 15875-4413, Tehran, Iran*

Received 21 December 2012; received in revised form 22 February 2013; accepted 12 March 2013
Available online 20 March 2013

Abstract

Due to the delayed and weak bone-implant integration in dental and orthopedic devices, there have been several attempts to enhance implant–bone interactions for rapid osseointegration. In this paper, the interactions of human bone marrow-derived stromal (mesenchymal) stem cells (hMSCs) with uncoated and coated titanium alloy implants with poorly crystalline apatite are studied. First the configuration and chemical composition of the apatite coatings and their deposition progress in different experimental conditions are investigated and discussed. Then, hMSCs are cultured on different substrates and cell attachment and proliferation are monitored and evaluated for different time intervals. Although the uncoated and coated substrates indicate good cell attachment, the differences in proliferation and morphology of the cells spread over the coated samples are significant. It is concluded that the coated samples improve the capability for accepting the cells in three-dimensional and slender shapes. The migration of hMSCs on both substrates are discussed. As such cell migration is directly associated to the osteoconduction, the findings confirm the hypothesis of enhancement in bone formation on the surface of biomimetically poorly crystalline apatite coated titanium implants. This *in vitro* study demonstrates that the coated samples are nontoxic and biocompatible enough for ongoing osteogenic studies in bone or dental defects in animal models *in vivo*.

Keywords: D: Apatite; Biomimetic technique; Bone marrow-derived human mesenchymal stem cells; Orthopedic and dental titanium implants

1. Introduction

Implantation of orthopedic and dental implants is affected by delayed or weak implant–bone integration and inadequate bone formation. Innovative approaches have been sought to improve the interaction between implant and bone to achieve rapid osseointegration. Among different alloys used for implantation, titanium alloys have become the most popular biomedical materials due to their biocompatibility, excellent corrosion resistance, good mechanical properties and lightness [1]. Titanium without any surface treatments is bioinert, not bioactive, and cannot bond directly to the surrounding bone tissues when implanted in the human body.

The surfaces of these implants are the sites where osseointegration occurs. Optimizing the surface characteristics of implants could promote the formation of newly formed bone and osseointegration. During the last years, many techniques have been employed to enhance the *in vivo* osseointegration of titanium-based implants such as physical machining and controlled oxidation [2,3]. Recently, biomimetic approach has been extensively used for improvement of titanium implants. An example is calcium phosphate coatings, such as hydroxyapatite, which is employed for surface modification of orthopedic and dental implants [4–6]. The addition of this highly bioactive material to the surface of oxidized metallic implants shows dramatic enhancement in bone bonding [7]. This hard tissue integration would lead to quicker patient recovery and extended life for orthopedic implants [8]. The bone-like calcium phosphate apatite coating is achieved by placing the substrates into SBF medium in body temperature and at the blood pH.

Generally, biomimetic approach has become a modern method to create bioactive surfaces in different conditions such as sodium hydroxide and/or heat-treatment [1,9], as well as hydrogen peroxide of titanium substrates treatment [10] besides various pretreatments

*Corresponding author. Tel./fax: +98 21 44580386.
E-mail addresses: sfaghihi@nigeb.ac.ir, shahabeddin.faghihi@mail.mcgill.ca (S. Faghihi).

0272-8842/$ - see front matter © 2013 Elsevier Ltd and Techna Group S.r.l. All rights reserved.
http://dx.doi.org/10.1016/j.ceramint.2013.03.039

[11,12]. Also, changing the SBF conditions [13,14] have been widely investigated *in vitro* and *in vivo* to optimize long-term stable interfaces between bone tissues and implants. As an important factor, crystallinity may affect the cell response. According to Shi et al. [15] crystallinity can modulate adsorption of adhesion ligands to the surface. In addition, Kim et al. [16,17] reported the production of poorly crystalline apatite thin film formed at low temperatures with similar crystallographic properties to that of natural bone. It seems that biomimetic approach might be a good way to prepare poorly crystalline coatings on the surface of metalic implants.

Hydroxyapatite is a naturally occurring mineral and the predominant mineral component of vertebrate bone and tooth enamel. Naturally-occurring bone mineral is made of nanometer sized and poorly-crystalline calcium phosphate with apatite structure [18]. The ideal stoichiometric crystalline hydroxyapatite, $Ca_{10}(PO_4)_6(OH)_2$, has the atomic Ca/P ratio 1.67 [19,20] but the composition of bone mineral is significantly different and can be represented by the following formula :

$$Ca_{8.3}(PO_4)_{4.3}(HPO_4,\ CO_3)_{1.7}(OH,\ CO_3)_{0.3} \quad (1)$$

Bone mineral is poorly-crystalline and non-stoichiometry due to the presence of divalent ions, such as CO_3^{2-} and HPO_4^{2-} which are substituted for the trivalent PO_4^{3-} ions. Substitution by CO_3^{2-} and HPO_4^{2-} ions produces a change of Ca/P ratios, resulting in the Ca/P ratios which may vary depending on the age and bone site [21]. It is worth to note that biomimetic approach has the ability to form such bone-like apatite. By this time, major factors which have been thought to have influence on cell behavior in case of calcium phosphate coatings were roughness, morphology, micro- and nano-structure, crystallinity, and chemical composition of the substrate [22–24]. However, the exact mechanism to explain the favorable effect of calcium phosphate coatings on bone response is still not clear. One of the features that were ignored in these studies was monitoring the cell and coating behavior during their interaction time which might help us to gain more knowledge about cell/calcium phosphate interface.

In this study, the surfaces of titanium implants were coated with thin films of poorly crystalline apatite through biomimetic approach. We monitored and analyzed the cell behavior consisting adhesion, proliferation and morphology during 15 days in comparison with uncoated implant samples. It is well-known that bone-related cells such as osteoblasts and bone marrow mesenchymal stem cells (BMSCs) play the most essential role in these biological mineralization processes [25,26]. Therefore, human mesenchymal stem cells (hMSCs) were chosen in this study. With our best knowledge hMSCs have never been examined in similar studies on poorly crystalline apatite coated titanium implants.

2. Materials and methods

2.1. Sample preparation

Commercially available Ti_6Al_4V titanium alloy (EZM Chiruline, Germany) (ASTM F136 and ISO 5832-3) samples were cut to appropriate sizes of 20 mm in diameter and 1 mm in thickness. The size of samples was checked with an electric digital caliper. Ti samples were initially polished with nos. 200–5000 grit silicon carbide (SiC) papers, and rinsed with acetone, ethanol and distilled water each for 10 min, respectively, and dried at 37 °C for 24 h.

2.2. Alkaline-treatment

The cleaned titanium samples were soaked into NaOH bath at the concentration of 5 M, and temperature of 60 °C in which they were treated for 1 day. Following the treatment, the samples were slowly washed with distilled water and dried at 40 °C in an electric oven overnight.

2.3. Heat-treatment

The Ti_6Al_4V alloy samples were alkaline treated with 5 M NaOH at 60 °C for 1 day, after which they were washed with distilled water and dried at 40 °C in an electric oven overnight. The samples were then heat-treated at 600 °C for 1 h in a Ni–Cr electrical furnace in air and then they were cooled down to ambient temperature in the furnace to avoid thermal shocks.

2.4. Preparation of SBF solution

The SBF solution was prepared by dissolving reagent-grade NaCl, KCl, $NaHCO_3$, $MgCl_2 \cdot 6H_2O$, $CaCl_2$ and KH_2PO_4 into distilled water and buffered at a pH 7.25 with trishydroxymethyl aminomethane (TRIS) and 1 N HCl solution at 37 °C. Its composition is given in Table 1 and compared with the human blood plasma. Note that SBF is a solution highly supersaturated with respect to apatite [27–30].

2.5. Biomimetic apatite deposition

We carried out *in vitro* studies by soaking the samples in SBF solution at 37 °C for 14 days to investigate the formation of biomimetic apatite on the surface of samples. To keep the ionic concentrations constant, SBF solution was refreshed every 2 days. At regular intervals, the samples were taken out and rinsed with double distilled water and dried in an oven.

Table 1
Ion concentrations of simulated body fluid (SBF) and human blood plasma.

Ion	Plasma (mmol/l)	SBF (mmol/l)
Na^+	142.0	142.0
K^+	5.0	5.0
Mg^{2+}	1.5	1.5
Ca^{2+}	2.5	2.5
Cl^-	103.0	147.8
HCO_3^-	27	4.2
HPO_4^{2-}	1.0	1.0
SO_4^{2-}	0.5	0.5

2.6. Sample characterization

2.6.1. X-ray diffraction (XRD) analysis

The phase composition of the samples' surfaces was analyzed by XRD with Siemens-Brucker D5000 diffractometer. This instrument works with voltage and current settings of 40 kV and 40 mA respectively and uses Cu-Kα radiation (1.540 Å). For qualitative analysis, XRD diagrams were recorded in the range of $10^\circ \leq 2\theta \leq 70^\circ$ at the scan speed of 2 deg/min.

2.6.2. Selected area electron diffraction (SAD) analysis

The ultrastructure of apatite formed on the substrates was analyzed by selected area electron diffraction (SAD) connected to a transmission electron microscopy (TEM: Philips CM200 model) operated at 200 kV. The samples for SAD analysis were prepared by careful removal of the reaction layer from the coating surface using razor blade.

2.6.3. Scanning electron microscopy (SEM) analysis

The surface morphology and microstructure of the samples were evaluated using SEM. The samples were coated with a thin layer of gold (Au) by sputtering (EMITECH K450X, England) and then the surface morphology of them were observed on a scanning electron microscope (SEM Philips XL30) that operated at the acceleration voltage of 15 kV.

2.6.4. Energy dispersive X-ray (EDX) analysis

Energy dispersive X-ray analyzer (EDX, Rontec, Germany) connected to SEM was used to investigate semi-quantitative chemical compositions.

2.7. Cell culture

In order to study and monitor the attachment, proliferation and morphology of hMSCs, the cell line was selected from the Cell Therapy Center of Royan Institute. Alfa Minimum Essential Media (α-MEM, Sigma, USA) supplemented with 10% Fetal Bovine Serum (FBS, Gibco, Taastrup, Denmark) and 1% antibiotic solution (Sigma, USA) was used as cell incubation medium. The cells were grown to confluency in controlled atmosphere condition (37 °C, 5% CO_2, 95% humidity). Detachment of confluent low passage cells was performed using 1.25% Trypsin/EDTA solution (Sigma, USA). Subsequently, hMSCs cells were cultured over several substrates in concentration of 5×10^4 cell/cm^2 and incubated for 1, 2 and 4 h in to study the cell attachment. In addition, cells were cultured over another series of substrates in concentration of 5×10^3 cell/cm^2 and incubated for 5, 10 and 15 days to study cell proliferation. Tissue culture grade polystyrene was used as the control, and replicates were prepared. After each incubation period, the samples were washed with Phosphate Buffer Saline (PBS, Sigma, USA) solution, and cell counting was performed in each period. Same samples were fixed in gluteraldehyde 2.5% for observation with SEM. After fixation, the samples were dehydrated in crescent ethanol concentrations (30%, 50%, 70%, 90%, 95%, and 100%).

2.8. Statistical analysis

All experiments were run in four replicates and repeated at least five separate times. All data are presented as the mean value ± standard deviation (SD) of each group. Statistical analysis was performed by using Student's *t*-test. For all tests of significance, a p value of 0.05 or less was considered statistically significant.

3. Result and discussion

3.1. XRD analysis

The XRD measurements were performed on the polished samples, before and after 7 and 14 days immersion in SBF. As it can be seen in Fig. 1(a), there are some small peaks of α-Ti and β-Ti which are in accordance with JCPDS files no. 44-1294 and 44-1288, respectively. Some studies showed that titanium is easily oxidized, and if Ti_6Al_4V is subjected to air at low temperatures, an oxide layer with a thickness of up to 10 nm may spontaneously form [1]. In spite of this, no additional phases could be detected in our recorded XRD patterns.

After 7 days of deposition, another set of weak peaks around $2\theta = 24^\circ$, 28°and 53° was observed, which was attributed to the presence of newly formed apatite. The small and weak peaks of apatite in XRD patterns indicated that the peaks were not clearly detectable. However, SEM observations showed clearly detectable apatite particles after the first days of immersion in SBF. According to Sepahvandi et al. [27], XRD is not a powerful technique for measurement of the newly formed apatite. In our previously published article, we studied the ability of biomimetic apatite deposition on the surface of titanium substrates in SBF by the inherent luminescence properties of apatite [27]. We reported that biomimetic apatite was formed within the first hours; however, the XRD patterns could not clearly detect it. There are two reasons for the formation of poorly crystallized amorphous apatite: first, the immersion time in SBF solution was not long enough to form well-structured apatite [31]; second, the SBF solution contains CO_3^{2-} and HPO_4^{2-} ions which might be substituted in the structure of apatite.

As it can be seen in Fig. 1, the substance formed on the surface of the treated samples became nearly detectable after 14 days immersion in SBF, and according to the standard JCPDS file no. 09-0432, the new weak peaks were assigned to be (0 0 2), (2 1 0), (2 1 1), (1 1 2), (3 0 0) and (3 1 2) reflections of biomimetic apatite phase. As expected, the XRD patterns from the coatings corresponded to apatite with coincident peak positions and low intensities, indicating a low signal-to-noise ratio (corresponding to a poorly crystalline apatite). Therefore, the small and broad peaks suggested the formation of apatite phase with small crystallites and/or defective structures which is nearly similar to the structure of bone-like apatite. The selected area electron diffraction (SAD) pattern of the apatite coating treated for 14 days in SBF solution is shown in Fig. 1(b). According to the powder

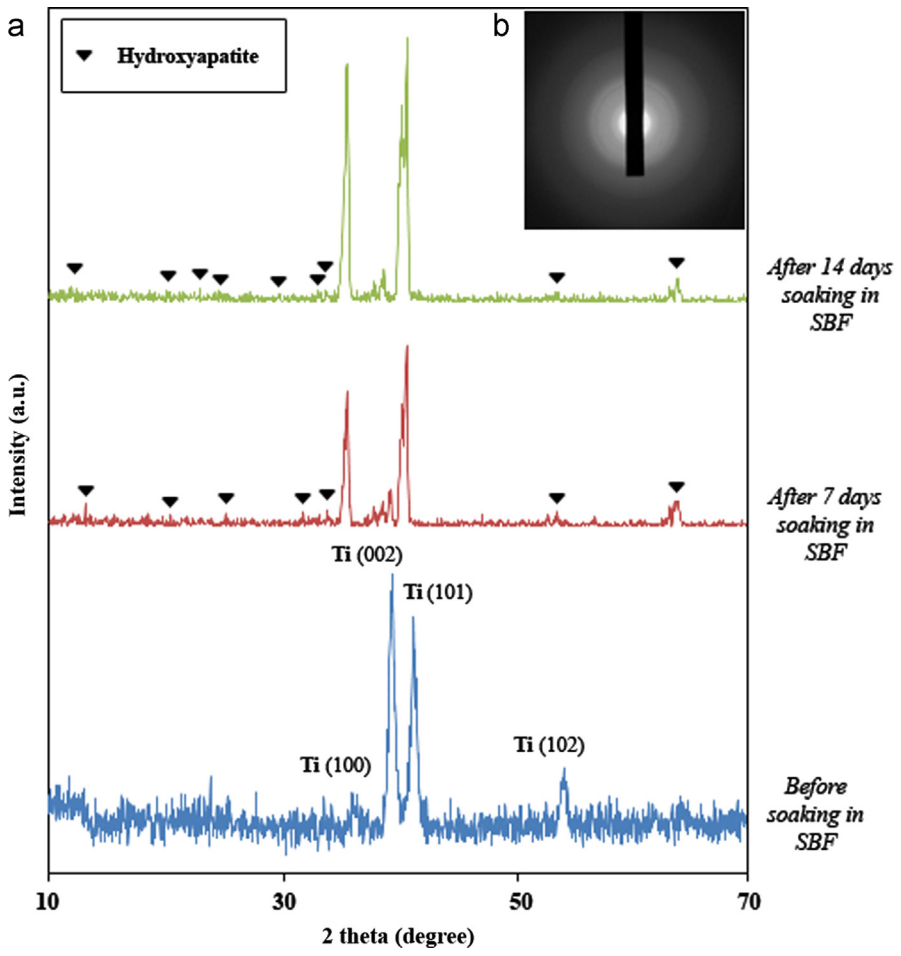

Fig. 1. (a) XRD pattern of the surface of titanium implants after alkaline-treatment before immersion, after 7 days and after 14 days immersion in SBF. (b) Selected area electron diffraction (SAD) pattern of the apatite layer treated for 14 days in SBF.

diffraction file no. 09-0432, the electron diffraction rings from the inner to the outer ring were matched to those of apatite but the diffuse and broad diffraction rings indicated that the apatite particles were formed with low crystallinity.

3.2. SEM observations

Fig. 2 shows the SEM micrographs of different untreated, treated, coated and uncoated samples. As it can be seen in Fig. 2(a) and (b), the treated Ti_6Al_4V substrates showed porous-like structure with tiny holes which is different from those of native and just polished Ti_6Al_4V substrates. After 7 days soaking in SBF, the surface of samples was partially covered by a layer of cauliflower particles as shown in Fig. 2 (c) and (d), which was characterized as a poorly crystalline calcium phosphate phase by XRD measurements. As seen in Fig. 2(e) the underlying surface was not observable after 14 days soaking in SBF, and the small cauliflower apatite crystals were densely packed. In addition, the SEM micrograph of the cross-section of coated sample showed that the thickness of the coating was approximately 4–5 μm. Note that the obtained spheroid morphology of particles are more beneficial than bar- or needle-like crystals when they are in contact with osteoblastic cells [32]. A possible explanation for this observed phenomenon is that the spherical particles can form a more tightly packed apatite layer than large bars or needles, and hence can present a continuous and smoother apatite surface to the proteins and cells [32].

3.3. EDS analysis

The formation of apatite layer on the surface of titanium implants was also confirmed by EDS analysis, as shown in Fig. 2(f). The EDX spectrum indicates the peaks of Ti, Al and V elements related to the titanium implant, and the peaks of P, Ca, and C corresponded to the newly formed apatite layer. These results confirmed the right composition of the newly formed apatite. Also, according to the Ca and P peaks of the EDX graph, the Ca–P molar ratio calculated in the range of 2.6 which we suspect is related to the nonstoichiometric hydroxy-carbonate apatite [33].

3.4. Cell adhesion

In *in vitro* cultures, cells do not feel the naked surfaces, but a layer of adsorbed ions, proteins and other molecules native from the culture medium covers the surfaces. Cell attachment

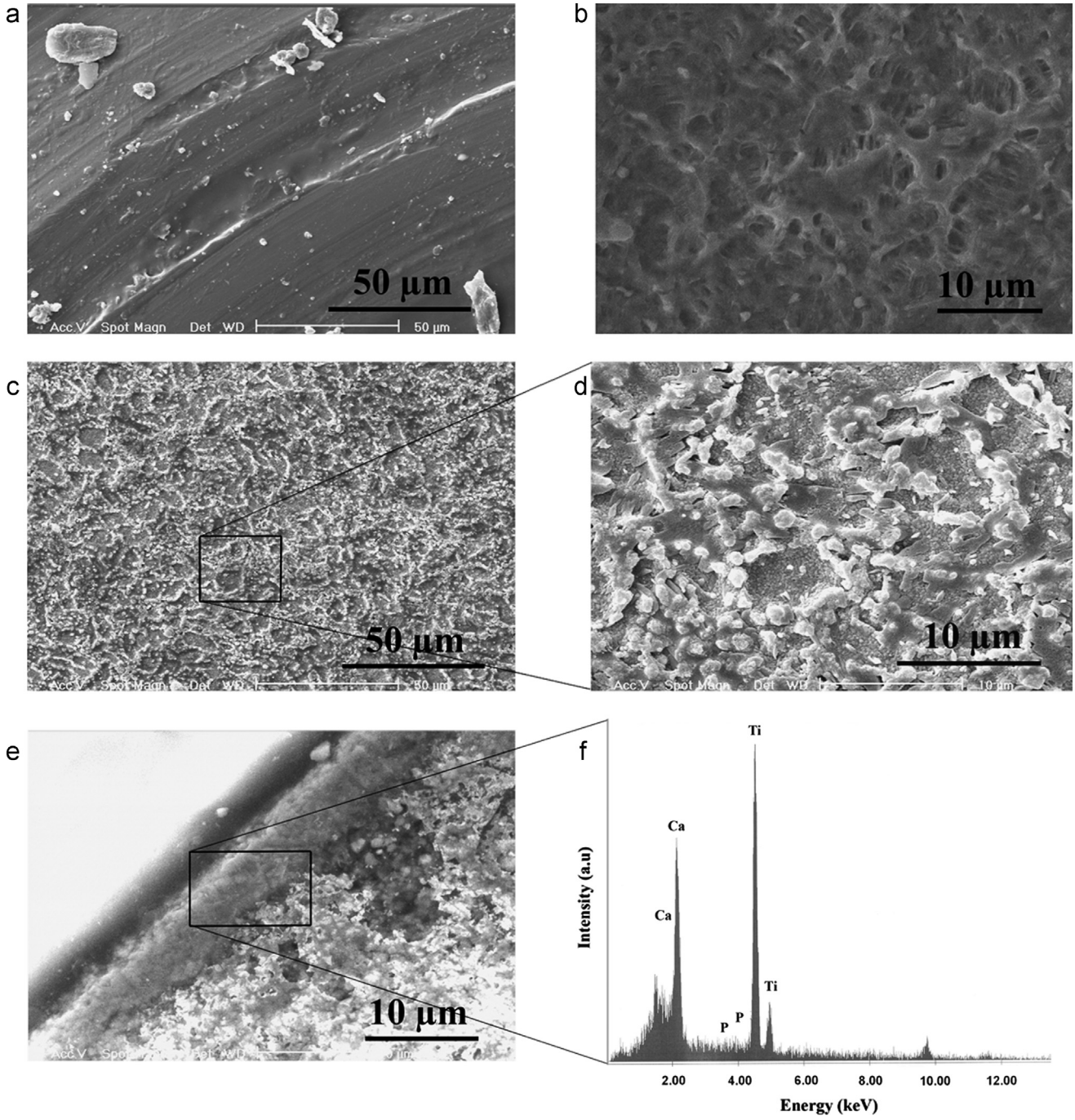

Fig. 2. SEM micrographs of the titanium implant surfaces: (a) untreated sample, (b) after alkaline-treatment, (c) after 7 days in SBF, (d) high magnification of the sample after 7 days in SBF, (e) cross-section of newly formed apatite layer after 14 days immersion in SBF, and (f) EDX pattern of the newly formed layer.

occurs via protein adhesion molecules in this layer. Especially, fibronectin and vitronectin present in the supplemented FBS, are known to promote cell adhesion and spreading on different materials such as apatite [34,35]. Here, cell adhesion test was used to evaluate the cytocompatibility of the prepared samples. As it can be seen in Fig. 3, the amount of cells attached to the surface of biomimetic apatite increases with increasing the incubation time (from 1 to 4 h) but there was no significant difference between the apatite coated samples and uncoated smooth titanium ones even after 4 h. Some studies reported higher cell attachment on hydroxyapatite than titanium substrates [36,37]. On the other hand, in the study of Puleo et al. [38] they showed an acceptable cell attachment can be formed on the surface of uncoated titanium samples. As mentioned earlier, cell attachment is mediated through proteins adsorbed into the substrate surface. Surprisingly, some studies argued differences in protein adsorption between apatite and titanium surfaces, whereas other ones did not report these differences [39,40]. The reason of these differences is not clearly understood.

In our study, there was statistically significant difference between the plain culture dish, coated and uncoated samples from the beginning. The hMSCs are attached to the plain

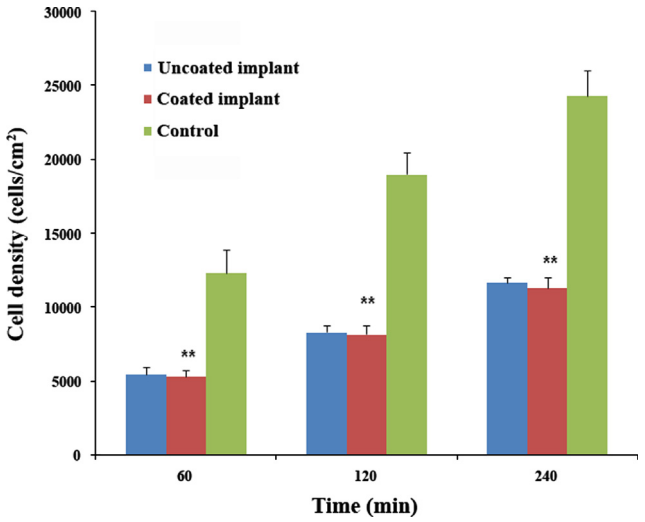

Fig. 3. Attachment of the hMSCs on the culture plate (control), coated and uncoated samples after culturing for 1, 2 and 4 h.

culture dish more quickly than the coated and uncoated samples. The obtained result is different from the data reported by Hong et al. [41] demonstrating higher cell adhesion to apatite than culture plate. They argued that it is due to the highest surface roughness, high concentration of labile ions in the biomimetic crystalline apatite crystals and high specific area due to the nanodimensional network in the highly crystalline apatite film, which may increase the reactivity of this thin film to the cells. Hong et al. [41] also claimed that more rapid adhesion of osteoblast cells might provide a better chance to take over the surface in a competition with the other cells because there must be a mixed cell environment when the biomaterial is inserted into the body. Note that this kind of initially high cell attachment might not be favorable in some cases. In fact, in real situation cell proliferation has a direct relationship with the initial cell attachment. As a result, cell proliferation should be considered as a key factor for cytocompatibility, which is needed to be evaluated in detail. Zhu and Assoian [42] reported that cells are required to spread on the surface in order to survive and proliferate, and adhesion was not the only factor for survival.

In another point for view, Bigerelle et al. [43] showed that when the topography is considered below the cell scale (microroughness), cells appreciate their isotropic smooth aspect. However, when the topography is above the cell scale (macro-roughness) they take advantage of their rough isotropic. In our study, qualitative observations suggested that the topography was below the cell scale. As a result, it seems that the cells appreciate their smooth surface which might justify this difference.

3.5. Cell proliferation

The growth of hMSCs with culturing time was observed on culture plate (control), coated and uncoated samples as shown in Fig. 4. The cell numbers multiplied significantly, reflecting the proliferation processes of the cells. Cell proliferation was nearly similar on all surfaces after 5 days of culture. However, the mean cell number that proliferated for 5 days on the coated and uncoated samples was slightly lower than that of the culture plate. In addition, a greater proliferation rate occurred between 10 and 15 days. The number of cells on the culture plate was significantly higher than those apatite coated and uncoated samples after 10 and 15 days. Moreover, the mean unit cell number for coated samples was statistically higher than those uncoated samples in 10 and 15 days of culturing. SBF treatment which led to the formation of poorly crystalline apatite on the surface of implants showed an incensement in cell adhesion and proliferation. Furthermore, various aspects have been reported repeatedly about physico-chemical properties of material surface which effected cell adhesion and proliferation [44]. As the crystallinity of apatite coating has a significant effect on the cell behavior, Frayssinet et al. [45] reported that highly crystalline surfaces might have an inhibitory effect on cell growth behavior.

On the other hand, DiMillia et al. [46] suggested that proliferation capacity and migration speed of various cell types, *e.g.* mesenchymal stem cells is in highest range at intermediate adhesion, while high adhesion capacity is associated with quiescence and maturation of cells [47,48]. Here, comparing with the initial cell density, a significant increase was observed in the amount of cells after 15 days of culture on all surfaces (at least three times as many as the seeding density).

3.6. Cell morphology

As it can be seen in Fig. 5, typical SEM micrographs showed the morphological features of hMSCs cultured on uncoated and coated samples for 1, 2 and 4 h. As shown in Fig. 5(a) and (b), after 1 h of cell culturing, spherical cells with early sign of filopodial extensions were observed on the surface of both uncoated and coated samples. Subsequently, 2 h after cell culturing, the cells in contact with uncoated samples were more intimate to the substrate than coated samples as shown in Fig. 5(c) and (d) for uncoated and coated

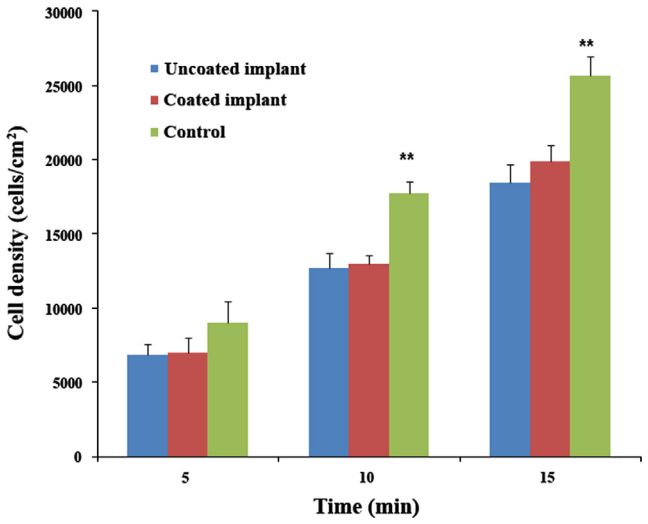

Fig. 4. Proliferation of the hMSCs on culture plate (control), coated and uncoated samples after culturing for 5, 10 and 15 days.

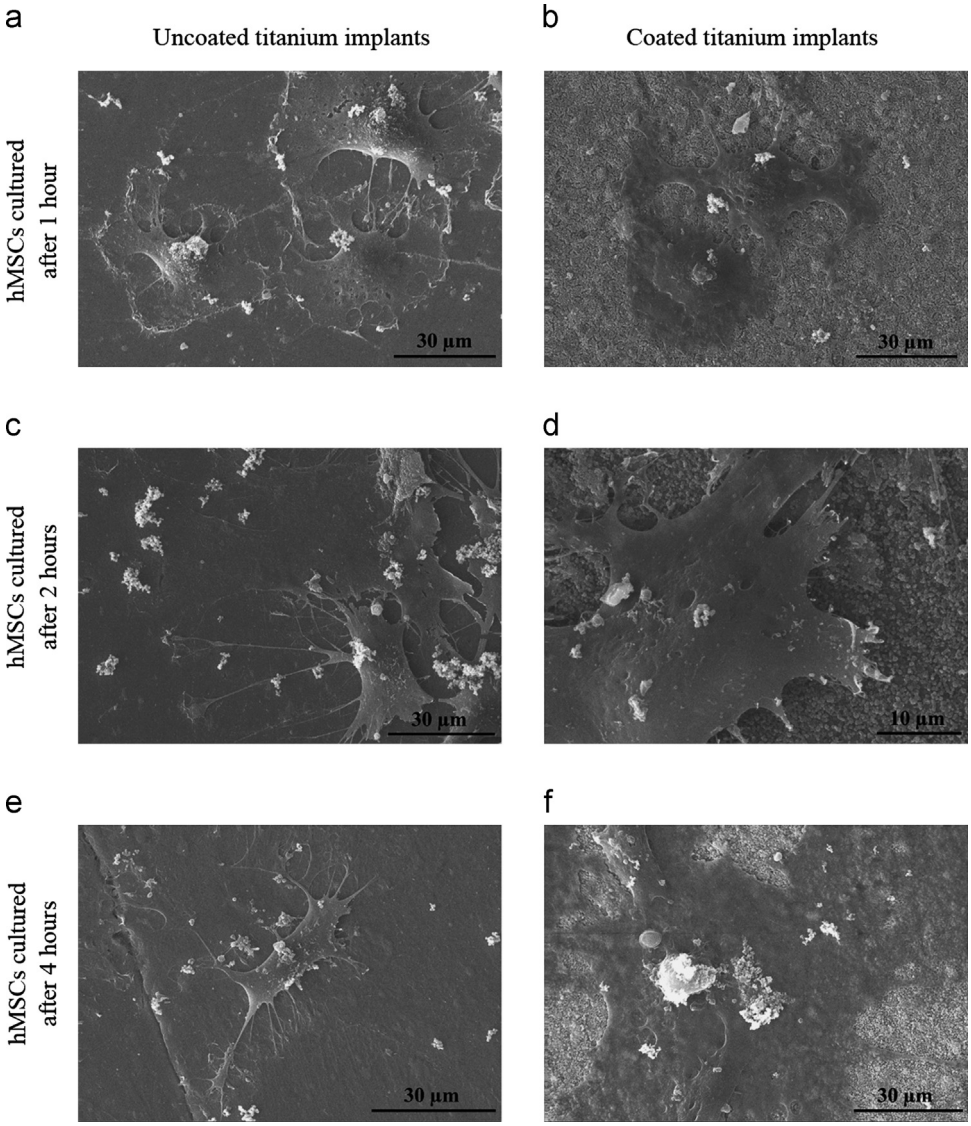

Fig. 5. SEM micrographs of hMSCs cultured on samples: (a) Uncoated and (b) coated samples for 1 h after cell culturing, (c) uncoated and (d) coated samples for 2 h after cell culturing, (e) uncoated and (f) coated samples for 4 h after cell culturing.

samples, respectively. After 4 h of culturing, the hMSCs appeared to be more flattened and spread as shown in Fig. 5(e) and (f) for uncoated and coated samples, respectively.

Obtained results indicated that the cultured cells on the surface of uncoated samples were spread with polygonal morphology, and the cellular filopodia anchored more tightly to the substrate. Whereas, coated samples showed less filopodia and the cell bodies appeared to stand off the surface.

Surprisingly, the difference on cell morphology was obvious from the first time of interaction. In our study, changes in cell morphology have been tracked after 5, 10 and 15 days of culturing as shown in Fig. 6. As it can be seen in Fig. 6(a) and (b), after 5 days non-spreading spherical cells were not observed on both uncoated and coated, respectively. Cells on the surface of uncoated samples were flat, elongated with well spread shape. After 10 days, the cells on the surface of coated samples were trying to elongate in one direction whereas cells on uncoated samples were spread in all directions as shown in Fig. 6(c) and (d). Subsequently, after 15 days, hMSCs were spread very well on the surface of uncoated samples. As a result, it was difficult to distinguish cells on the substrates (see Fig. 6(e) and (f)) whereas the cells were almost slender in shape and more three-dimensional on the surface of coated samples [49].

The appearance of more slender cells on the surface of coated samples may increase the possibility of cells migration. It can be concluded that the less spread cells could migrate more rapidly than widely spread cells. Too much adhesion hinders the movement of cells over the surface [50]. The migration of osteoblast cells are directly related to the osteoconduction which indicates the advancement of bone formation via the solid surface of biomaterials [51]. Therefore, it is believed that more the slender cells on the coated samples may exhibit signs of higher osteoconduction. Accordingly, Folkman and Moscona [52] mentioned that one of the main regulators of proliferation rate in anchorage-dependent cells is

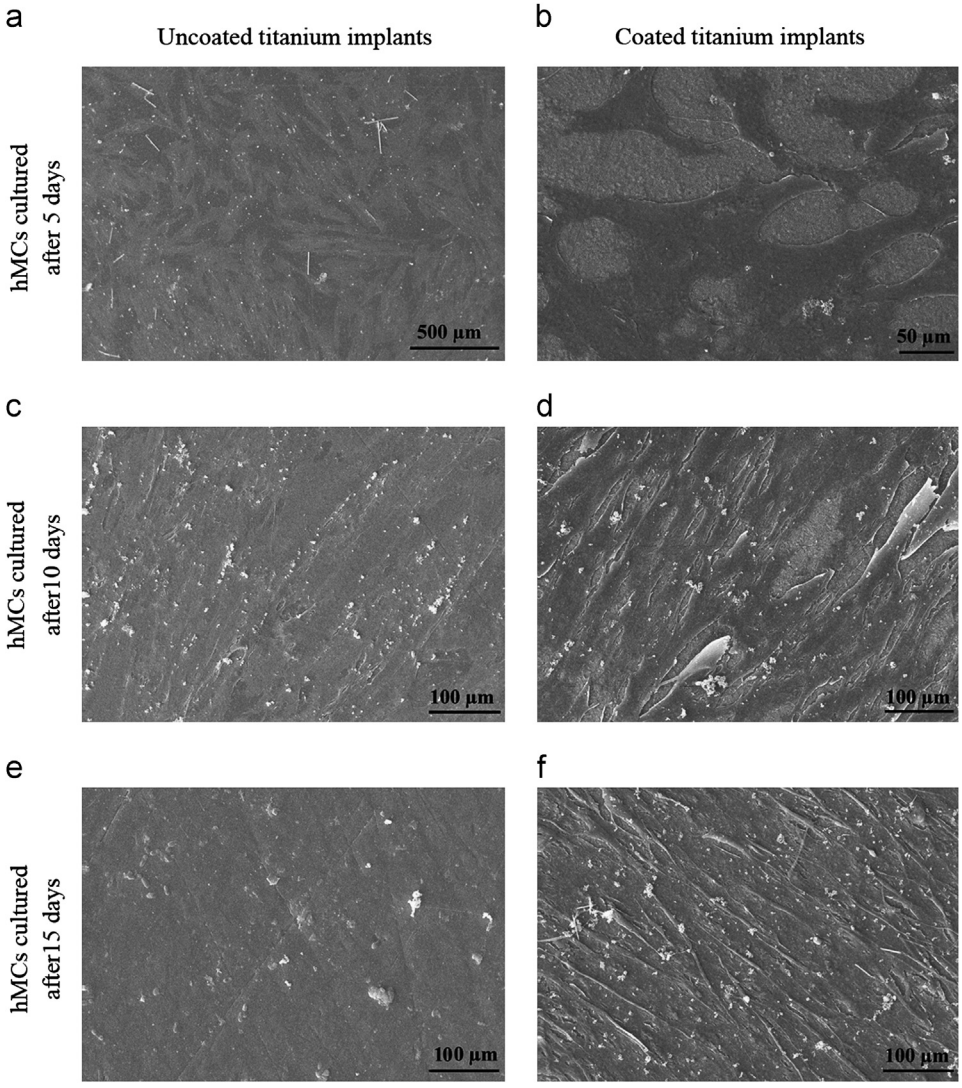

Fig. 6. SEM micrographs of hMSCs cultured on samples: (a) Uncoated and (b) coated samples for 5 days after cell culturing, (c) uncoated and (d) coated samples for 10 days after cell culturing, (e) uncoated and (f) coated samples for 15 days after cell culturing.

the shape of cells. Their results indicate that cells in round configuration divide at a lower rate than the flattened and well-spread cells.

It may be also possible that the surface topology of coated apatite would be responsible for cell behavior. However, Rice et al. [53] studied the response of human osteoblast cells on Ti oxide substrate, and concluded that the surface chemistry is a more dominant factor than topography. It seems that the surfaces of coated and uncoated samples differed by more than just surface chemistry. Specifically, it is likely that the surface topography and roughness values may be differed. We did not include a roughness control group because we predicted that the apatite coating would be changed during 14 days in contact with cells and culture medium.

It is worth mentioning that dissolution and formation of apatite layer can happen simultaneously on the surface of samples in culture medium. Here, after putting the coated samples in α-MEM some interaction might happen in the surrounding area which can be described as follows: (a) release of calcium and phosphate ions from the coating, (b) ion exchange with surrounding medium and (c) precipitation of newly apatite crystals. It can be seen from the SEM micrographs that spherical particles which were recognized as biomimetic apatite were stable from 1 h to 14 days in culture medium. Faure et al. [54] also used an acellular DMEM solution as a biomimicking medium instead of SBF solution, and observed the formation of this newly formed apatite.

On the other hand, the pH of the culture medium was measured every 3 days which was in the range of 7.0–8.0. This suggested that, the pH of culture medium was not affected by the presence of the coating and remained almost equal to the pH of the culture medium (7.67 ± 0.06). Barrere et al. [55] reported that even a slightly acidic condition can induce the dissolution of apatite layer and the release of Ca^{2+} and PO_4^{3-} ions into the extracellular environment. Large amount of ion release from the apatite coating may create a microenvironment surrounding the cell in which the levels of Ca^{2+} and PO_4^{3-} are toxic. Our results confirmed that the culture conditions did not cause a noticeable release of ions from the coating into the solution. The presence of an adsorbed

protein layer might be sufficient for preventing Ca^{2+} and PO_4^{3-} uptake by cells. On the other hand, the apatite dissolution could be significantly affected by protein adsorption, conformation and modulation [56,57].

4. Conclusion

In this research, the hMSCs–implant interactions of uncoated and biomimetically coated titanium implants have been investigated. After the first day of immersion in SBF, the partially amorphous apatite particles exhibited the typical cauliflower like morphology. It could be concluded that both of the coated and uncoated substrates had good cell attachment. However, proliferation and morphology of the hMSCs spread over the coated substrates differed significantly from that of the uncoated one. Also, the coated substrates were more prone to cell formation in three-dimensional and slender shape than the uncoated ones. This work has shown that the applied apatite coating on the titanium implants can improve the biological response of hMSCs, while the desirable bulk characteristics of the substrates are retained.

Acknowledgments

We gratefully acknowledge the financial support of this work by Tissue Engineering and Biomaterials Division, National Institute of Genetic Engineering and Biotechnology (NIGEB).

References

[1] M. Long, H.J. Rack, Titanium alloys in total joint replacement—a materials science perspective, Biomaterials 19 (18) (1998) 1621–1639.
[2] K.C. Baker, M.A. Anderson, S.A. Oehlke, A.I. Astashkina, D.C. Haikio, J Drelich, et al., Growth, characterization and biocompatibility of bone-like calcium phosphate layers biomimetically deposited on metallic substrata, Material Science and Engineering C 26 (2006) 1351–1360.
[3] F. Barrere, C.A. Van Blitterswijk, K. de Groot, P. Layrolle, Influence of ionic strength and carbonate on the Ca–P coating formation from SBFx5 solution, Biomaterials 23 (2002) 1921–1930.
[4] H. Li, W.Y. Huang, Y.M. Zhang, M. Zhong, Biomimetic synthesis of enamel-like hydroxyapatite on self-assembled monolayers, Material Science and Engineering C 27 (2007) 756–761.
[5] T. Kokubo, H.M. Kim, M. Kawashita, T. Nakamura, Bioactive metals: preparation and properties, Journal of Materials Science 15 (2004) 99–107.
[6] S.A. Poursamar, M. Azami, M. Mozafari, Controllable synthesis and characterization of porous polyvinyl alcohol/hydroxyapatite nanocomposite scaffolds via an in situ colloidal technique, Colloids and Surfaces B: Biointerfaces 84 (2011) 310–316.
[7] M. Demircioglu, A. Pasinli, R.S. Aksoy, H. Yildiz, I. Ozdemir, N. Arda, Fabrication and mechanical behavior of calcium-phosphate in situ coating on Ti_6Al_4V substrates, Key Engineering Materials 264–268 (2004) 2103–2106.
[8] R. Kamalian, A. Yazdanpanah, F. Moztarzadeh, R. Ravarian, Z. Moztarzadeh, M. Tahmasbi, M. Mozafari, Synthesis and characterization of bioactive glass/forsterite nanocomposites for bone implants, Ceramics—Silikáty 56 (4) (2012) 331–340.
[9] X.X. Wang, S. Hayakawa, K. Tsuru, A. Osaka, A comparative study of *in vitro* apatite deposition on heat-, H_2O_2-, and NaOH-treated titanium surfaces, Journal of Biomedical Materials Research 54 (2) (2001) 172–178.
[10] C. Ohtsuki, H. Iida, S. Hayakawa, A. Osaka, Bioactive of titanium treated with hydrogen peroxide solutions containing metal chlorides, Journal of Biomedical Materials Research 35 (1997) 39–47.
[11] K. Cai, M. Lai, W. Yang, R. Hu, R. Xin, Q. Liu, K.L. Sung, Surface engineering of titanium with potassium hydroxide and its effects on the growth behavior of mesenchymal stem cells, Acta Biomaterialia 6 (6) (2010) 2314–2321.
[12] A. Bigi, E. Boanini, B. Bracci, A. Facchini, S. Panzavolta, F. Segatti, L. Sturba, Nanocrystalline hydroxyapatite coatings on titanium: a new fast biomimetic method, Biomaterials 26 (2005) 4085–4089.
[13] A.C. Tas, S.B. Bhaduri, Rapid coating of Ti_6Al_4V at room temperature with a calcium phosphate solution similar to 10 × simulated body fluid, Journal of Materials Research 19 (2004) 2472–2479.
[14] A. Oyane, K. Onuma, A. Ito, H.M Kim, T. Kokubo, T. Nakamura, Formation and growth of clusters in conventional and new kinds of simulated body fluids, Journal of Biomedical Materials Research: Part A 64 (2003) 339–348.
[15] D. Shi, G. Jiang, J. Bauer, The effect of structural characteristics on the *in vitro* bioactivity of hydroxyapatite, Journal of Biomedical Materials Research 63 (1) (2002) 71–78.
[16] H.M. Kim, Y.S. Kim, K.M. Woo, S.J. Park, C. Rey, Y. Kim, J.K. Kim, J. S. Ko, Dissolution of poorly crystalline apatite crystals by osteoclasts determined on artificial thin-film apatite, Journal of Biomedical Materials Research 56 (2001) 250–260.
[17] H.M. Kim, Y. Kim, S.J. Park, C. Rey, H.M. Lee, M.J. Glimcher, J.S. Ko, Thin film of low-crystalline calcium phosphate apatite formed at low temperature, Biomaterials 21 (2000) 1129–1134.
[18] W. Neuman, M. Neuman, The Chemical Dynamics of Bone Mineral, University of Chicago, IL, 1958 34 pp.
[19] M. Azami, S. Jalilifiroozinezhad, M. Mozafari, Calcium fluoride/hydroxyfluorapatite nanocrystals as novel biphasic solid solution for tooth tissue engineering and regenerative dentistry, Key Engineering Materials 493–494 (2012) 626–631.
[20] N. Nezafati, F. Moztarzadeh, S. Hesaraki, M. Mozafari, A. Samadikuchaksaraei, L. Hajibaki, M. Gholipour, Effect of silver concentration on bioactivity and antibacterial properties of SiO_2–CaO–P_2O_5 sol–gel derived bioactive glass, Key Engineering Materials 493–494 (2012) 74–79.
[21] M. Mozafari, F. Moztarzadeh, Novel porous gelatin/bioactive glass scaffolds with controlled pore structure engineered via compound techniques for bone tissue engineering, in: Proceedings of the 1st Middle East Conference on Biomedical Engineering, MECBME, 2011, http://dx.doi.org/10.1109/MECBME.2011.5752076.
[22] C. Aparicio, D. Rodriguez, et al., Variation of roughness and adhesion strength of deposited apatite layers on titanium dental implants, Materials Science and Engineering C 31 (2) (2011) 320–324.
[23] Q. Hu, Z. Tan, et al., Effect of crystallinity of calcium phosphate nanoparticles on adhesion, proliferation, and differentiation of bone marrow mesenchymal stem cells, Journal of Materials Chemistry 17 (44) (2007) 4690–4698.
[24] M. Jafarkhani, A. Fazlali, F. Moztarzadeh, Z. Moztarzadeh, M. Mozafari, Fabrication and characterization of PLLA/chitosan/nano calcium phosphate scaffolds by freeze casting technique, Industrial and Engineering Chemistry Research 51 (2012) 9241–9249.
[25] P. Bianco, M. Riminucci, S. Gronthos, P.G. Robey, Bone marrow stromal stem cells: nature, biology, and potential applications, Stem Cells 19 (2001) 180–192.
[26] J.R. Mauney, V. Volloch, D.L. Kaplan, Role of adult mesenchymal stem cells in bone tissue engineering applications: current status and future prospects, Tissue Engineering 11 (2005) 787–802.
[27] A. Sepahvandi, F. Moztarzadeh, et al., Photoluminescence in the characterization and early detection of biomimetic bone-like apatite formation on the surface of alkaline-treated titanium implant: state of the art, Colloids and Surfaces B: Biointerfaces 86 (2) (2011) 390–396.
[28] M. Mozafari, M. Rabiee, M. Azami, S. Maleknia, Biomimetic formation of apatite on the surface of porous gelatin/bioactive glass nanocomposite scaffolds, Applied Surface Science 257 (2010) 1740–1749.
[29] A. Hamlekhan, M. Mozafari, N. Nezafati, M. Azami, H. Hadipour, A proposed fabrication method of novel PCL–GEL–HAp nanocomposite scaffolds for bone tissue engineering applications, Advanced Composite Letters 19 (2010) 123–130.
[30] A. Oyane, H.M. Kim, T. Furuya, T. Kokubo, T. Miyazaki, T. Nakamura, Preparation and assessment of revised simulated body fluids, Journal of Biomedical Materials Research 65A (2003) 188–195.

[31] L. Clèries, J.M. Fernández-Pradas, J.L. Morenza, Behavior in simulated body fluid of calcium phosphate coatings obtained by laser ablation, Biomaterials 21 (2001) 1861–1865.
[32] Z. Shi, X. Huang, Y. Cai, R. Tang, D. Yang, Size effect of hydroxyapatite nanoparticles on proliferation and apoptosis of osteoblast-like cells, Acta Biomaterialia 5 (1) (2009) 338–345.
[33] F. Baghbani, F. Moztarzadeh, A. Gafari Nazari, A.H. Razavi Kamran, F. Tondnevis, N. Nezafati, M. Gholipourmalekabadi, M. Mozafari, Biological response of biphasic hydroxyapatite/tricalcium phosphate scaffolds intended for low load-bearing orthopaedic applications, Advanced Composites Letters 21 (2012) 16–24.
[34] R.L. Juliano, Signal transduction by cell adhesion receptors and the cytoskeleton: functions of integrins, cadherins, selectins, and immunoglobulin-superfamily members, Annual Review of Pharmacology and Toxicology 42 (2002) 223–283.
[35] K.L. Kilpadi, P.L. Chang, S.L. Bellis, Hydroxyapatite binds more serum proteins, purified integrins, and osteoblast precursor cells than titanium or steel, Journal of Biomedical Materials Research 57 (2) (2001) 258–267.
[36] Y.-L. Chang, C.M. Stanford, J.S. Wefel, J.C. Keller, Osteoblastic cell attachment to hydroxyapatite-coated implant surfaces *in vitro*, International Journal of Oral and Maxillofacial Implants 14 (1999) 239–247.
[37] K. Okamoto, T. Matsuura, R. Hosokawa, Y. Akagawa, RGD peptides regulate the specific adhesion scheme of osteoblasts to hydroxyapatite but not to titanium, Journal of Dental Research 77 (1998) 481–487.
[38] D.A. Puleo, L.A. Holleran, R.H. Doremus, R. Bizios, Osteoblast responses to orthopedic implant materials *in vitro*, Journal of Biomedical Materials Research 25 (1991) 711–723.
[39] T. Matsuura, R. Hosokawa, K. Okamoto, T. Kimoto, Y. Akagawa, Diverse mechanisms of osteoblast spreading on hydroxyapatite and titanium, Biomaterials 21 (2000) 1121–1127.
[40] J.E. Ellingson, A study on the mechanism of protein adsorption to TiO_2, Biomaterials 12 (1991) 593–596.
[41] J.Y. Hong, Y.J. Kim, H.W. Lee, Osteoblastic cell response to thin film of poorly crystalline calcium phosphate apatite formed at low temperatures, Biomaterials 24 (18) (2003) 2977–2984.
[42] X.Y. Zhu, R.K. Assoian, Integrin-dependent activation of MAP kinase: a link to shape-dependent cell proliferation, Molecular Biology of the Cell 6 (1995) 273–282.
[43] M. Bigerelle, K. Anselme, et al., Improvement in the morphology of Ti-based surfaces: a new process to increase *in vitro* human osteoblast response, Biomaterials 23 (7) (2002) 1563–1577.
[44] L. Chou, B. Marek, W.R. Wagner, Effects of hydroxylapatite coating crystallinity on biosolubility, cell attachment efficiency and proliferation *in vitro*, Biomaterials 20 (1999) 977–985.
[45] P. Frayssinet, F. Tourenne, N. Rouquet, P. Conte, C. Delga, G. Bonel, Comparative biological properties of HA plasma-sprayed coatings having different crystallinities, Journal of Materials Science: Materials in Medicine 5 (1994) 11–17.
[46] P.A. DiMillia, J.A. Stone, J.A. Quinn, S.M. Albelda, D.A. Lauffenburger, Maximalmigration of human smooth muscle cells on fibronectin and type IV collagen occurs at an intermediate attachment strength, Journal of Cell Biology 122 (3) (1993) 729–737.
[47] B.K. Mann, J.L. West, Cell adhesion peptides alter smooth muscle cell adhesion, proliferation, migration, and matrix protein synthesis on modified surfaces and in polymer scaffolds, Journal of Biomedical Materials Research 60 (1) (2002) 86–93.
[48] L. Bacakova, L. Grausova, M. Vandrovcova, J. Vacik, A. Frazcek, S. Blazewicz, et al., Carbon nanoparticles as substrates for cell adhesion and growth, in: S.L. Lombardi (Ed.), Nanoparticles: New Research, Nova Science Publishers In., New York, 2008, pp. 39–107.
[49] K. Anselme, M. Bigerelle, B. Noel, E. Dufresne, D. Judas, A. Iost, et al., Qualitative and quantitative study of human osteoblast adhesion on materials with various surface roughness, Journal of Biomedical Materials Research 49 (2000) 155–166.
[50] S. Liu, M. Slepak, M.H. Ginsberg, Binding of paxillin to the alpha 9 integrin cytoplasmic domain inhibits cell spreading, Journal of Biological Chemistry 276 (2001) 37086–37092.
[51] A. Boyde, A. Corsi, R. Quarto, R. Cancedda, P. Bianco, Osteoconduction in large macroporous hydroxyapatite ceramic implants: evidence for a complementary integration and disintegration mechanism, Bone 24 (1999) 579–589.
[52] J. Folkman, A. Moscona, Role of cell shape on growth control, Nature 273 (1978) 345–349.
[53] J.M. Rice, J.A. Hunt, J.A. Gallagher, P. Hanarp, D.S. Sutherland, J. Gold, Quantitative assessment of the response of primary derived human osteoblasts and macrophages to a range of nanotopography surfaces in a single culture model *in vitro*, Biomaterials 24 (2003) 4799–4818.
[54] J. Faure, A. Balamurugan, et al., Morphological and chemical characterisation of biomimetic bone like apatite formation on alkali treated Ti_6Al_4V titanium alloy., Materials Science and Engineering C 29 (4) (2009) 1252–1257.
[55] F. Barrere, C.A. van Blitterswijk, K. de Groot, Bone regeneration: molecular and cellular interactions with calcium phosphate ceramics, International Journal of Nanomedicine 1 (2006) 317–332.
[56] M. Jafarkhani, A. Fazlali, F. Moztarzadeh, M. Mozafari, Mechanical and structural properties of polylactide/chitosan scaffolds reinforced with nano calcium phosphate, Iranian Polymer Journal 10 (2012) 713–720.
[57] A. Hamlehkhan, M. Mozafari, N. Nezafati, M. Azami, A. Samadikuchaksaraei, Novel bioactive poly(ε-caprolactone)–gelatin–hydroxyapatite nanocomposite scaffolds for bone regeneration, Key Engineering Materials 493–494 (2012) 909–915.